

**REPORT DOCUMENTATION PAGE**

Form Approved  
OMB No. 0704-0188

The public reporting burden for this collection of information is estimated to average 1 hour per response, including the time for reviewing instructions, searching existing data sources, gathering and maintaining the data needed, and completing and reviewing the collection of information. Send comments regarding this burden estimate or any other aspect of this collection of information, including suggestions for reducing the burden, to the Department of Defense, Executive Service Directorate (0704-0188). Respondents should be aware that notwithstanding any other provision of law, no person shall be subject to any penalty for failing to comply with a collection of information if it does not display a currently valid OMB control number.

**PLEASE DO NOT RETURN YOUR FORM TO THE ABOVE ORGANIZATION.**

<b>1. REPORT DATE (DD-MM-YYYY)</b> 18-06-2009		<b>2. REPORT TYPE</b> Final Report		<b>3. DATES COVERED (From - To)</b> 1 Sep 2007 - 31 Jul 2008	
<b>4. TITLE AND SUBTITLE</b> Specialty Fibers for Clinical Applications				<b>5a. CONTRACT NUMBER</b>	
				<b>5b. GRANT NUMBER</b> FA9550-05-1-0107	
				<b>5c. PROGRAM ELEMENT NUMBER</b>	
<b>6. AUTHOR(S)</b> Morse, Theodore F				<b>5d. PROJECT NUMBER</b>	
				<b>5e. TASK NUMBER</b>	
				<b>5f. WORK UNIT NUMBER</b>	
<b>7. PERFORMING ORGANIZATION NAME(S) AND ADDRESS(ES)</b> Trustees of Boston University 881 Commonwealth Avenue Boston, MA 02215				<b>8. PERFORMING ORGANIZATION REPORT NUMBER</b>	
<b>9. SPONSORING/MONITORING AGENCY NAME(S) AND ADDRESS(ES)</b> AFOSR 875 N. Randolph St, Room 3112 Arlington, VA 22203				<b>10. SPONSOR/MONITOR'S ACRONYM(S)</b> AFOSR/PKA	
				<b>11. SPONSOR/MONITOR'S REPORT NUMBER(S)</b>	
<b>12. DISTRIBUTION/AVAILABILITY STATEMENT</b> Approved for Public Release; Distribution Unlimited					
<b>13. SUPPLEMENTARY NOTES</b>					
<b>14. ABSTRACT</b> We have supplied fibers for confocal microscopy for the Wellman Institute at Harvard, such that we have a guiding core and a cladding around it that satisfies a specific numerical aperture. We have also done preliminary work on a HD x-ray that uses collimated bundles, in that they have nanoscale scintillating ceramics in the cores of the fibers. Fundamental problems in PMB (Polarization Mode Bearing) will be explored, in that they can provide a more sensitive measure of optical fiber performance.					
<b>15. SUBJECT TERMS</b>					
<b>16. SECURITY CLASSIFICATION OF:</b>			<b>17. LIMITATION OF ABSTRACT</b> SAR	<b>18. NUMBER OF PAGES</b>	<b>19a. NAME OF RESPONSIBLE PERSON</b> AFOSR
<b>a. REPORT</b> U	<b>b. ABSTRACT</b> U	<b>c. THIS PAGE</b> U			<b>19b. TELEPHONE NUMBER (Include area code)</b>

**Final Report**  
**Clinical Applications of Specialty Fibers, and**  
**novel biomedical Photonic concepts**  
**(AFOSR Award # FA9550-05-1-0107)**  
**T.F. Morse**  
**Laboratory for Lightwave Technology**  
**ECE/the Photonics Center, Boston University**

**Introduction**

Clinical and bio-photonics research will be carried out at the Laboratory for Lightwave Technology at Boston University in cooperation with the staff and faculty of the Wellman Institute for Photomedicine at MGH/Harvard. One of our responsibilities will be as advisor/consultant/colleague to the staff of the Wellman Institute on all matters associated with applications of optical fibers in the medical sciences. The following areas will be highlighted.

- A. Specialty fibers for clinical applications**
- B. High definition x-ray detection for medical imaging**
- C. PMB (Polarization Mode Beating) techniques in biodetection.**

**A. Specialty fibers for clinical applications.**

**i. Fibers for Confocal Microscopy**

We will continue development of specialty double clad optical fibers with Guillermo J. Tearney, M.D. This work was a focal point of a Ph.D. thesis by Caroline Boudoux, and the fiber from this effort is to be used in clinical studies involving confocal microscopy within the next year. The object of this fiber design was to provide greater resolution and simplicity in confocal microscopy. In a double-clad fiber, the design is such that a single mode core is surrounded by a multimode outer cladding that is traditionally the MCVD substrate tube itself. This is then coated with a low index polymer so that the region between the single mode core and the low index polymer serves as a multimode light guide. For commercially available fibers, the core is typically of the order of 8-10  $\mu\text{m}$ , and the outer diameter is 125  $\mu\text{m}$ . For confocal measurements, this small ratio ( $\lambda_{\text{core}}/\lambda_{\text{cladding}}$ ) results in image degradation. We have fabricated fibers with a much larger  $\lambda_{\text{core}}/\lambda_{\text{cladding}}$  ratio, and these have shown significant promise in simplifying the interpretation of confocal microscopy images.

**ii. Raman fibers for clinical applications**

If a laser interacts with tissue, there is a specific back scattered Raman signal. It has been discovered that fibrous plaque (good) in the coronary artery has a different Raman signal from fatty plaque (bad). This may be a predictor for stroke or heart attack. In order to make this measurement, it is necessary to put a fiber in the coronary arteries that places severe conditions on bending (as small as 7 mm), and on Raman effects induced in the fiber itself that masks the back scattered signal from the tissue. We are examining fibers that may be suitable for this application.

The problem with using a silica fiber to transmit the laser radiation and monitor the back scattered Raman signal from the tissue, is that there is a large Raman signature from the silica that masks the Raman signal from the tissue. Various filtering techniques

have been proposed. We have investigated the use of a PMMA fiber, where there is a slight “window” to allow the Raman tissue signature to propagate back to the detector. These have been unsuccessful in that the window that is required is highly absorbing.

### B. High definition x-ray detection for medical imaging

I made contact with Dr. Rox Anderson, who put me in touch with Dr. Raj Gupta, who is the expert on x-ray imaging in the radiology department at MGH. The concept will be described below, but we are pursuing an idea by which it might be possible to increase the resolution of x-ray imaging by an order of magnitude, i.e., from about 15  $\mu\text{m}$  to the order of 1  $\mu\text{m}$ .

When x-rays go through an object, they are scattered and absorbed. This density pattern can be monitored through traditional use of special film, or, in more recent advances, the information can be digitally recorded. The most convenient techniques for digital recording are to have the x-rays pass through the object being interrogated, and then onto a phosphorescent screen or crystal that produces visible photons. The intensity distribution of these visible photons is then subsequently detected with a dense CMOS array.

It is clear from this depiction shown in Figure 1 that resolution will be impaired by several factors, one of them being the finite thickness of the phosphorous screen, and the fact that the visible photons will have an angular distribution around the source of the scintillation photons. Thus, the visible photons will not impinge upon the CMOS pixel directly below. This problem can be significantly improved by placing the phosphorous screen, or the scintillating crystal on top of a collimated fiber bundle that guides the visible photons to the detector array. Indeed, were the phosphorous screen to be infinitely thin, the cross talk would be eliminated. Clearly this is not possible.

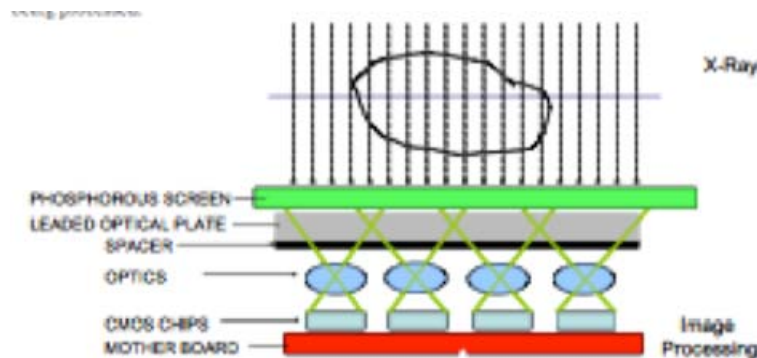


**Figure 1. CMOS detection array for digital x-ray imaging**

The collimating bundle for the visible light can be fabricated as follows, and they are commercially available from several sources. Imagine an optical fiber preform of several cm in diameter, with a large core of refractive index  $n_1$  surrounded by a cladding with a refractive index  $n_2$ , where  $n_1 > n_2$ . This preform is then drawn into cane, for example, with a size reduction of a factor of 10. These canes are then rebundled to make a bundled preform as large as the initial single preform. If this process is repeated 4 times, there is a 10,000 reduction in the size of the guiding core. This then the order of

resolution of the final bundle. In Figure 2, we show a bundle fabricated by Schott Glass of "soft glass". where each bright "pixel" has a diameter of 8 micron.

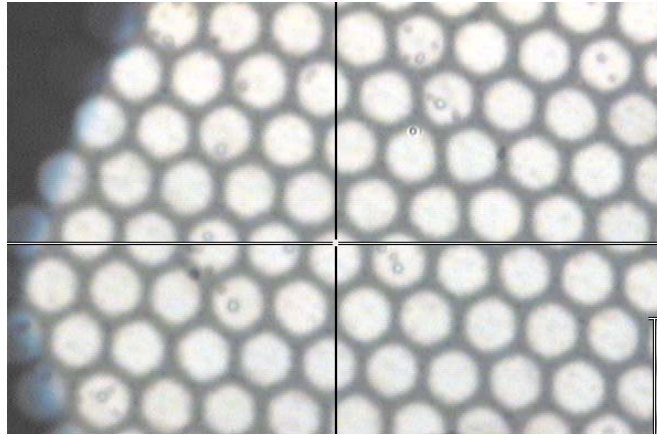


**Figure 2. Schott Glass coherent bundle, each "pixel" is 8 micron**

The scintillating layer will have a given thickness, that even if "thin" will be orders of magnitude larger than the pixel separation. For this reason, a collimating bundle placed directly below the scintillating material will not completely solve the problem of "cross talk". Only if the scintillation were to occur within the fiber bundle itself, would resolution be significantly enhanced. Indeed, one type of detection system grows NaI columnar scintillating microcrystals on top of each pixel of the detector array; however, this is a complex process, and the material is hygroscopic. It would be better to have a scintillating material as the core of a high index guiding structure. This can not be done with scintillating crystalline material; however, Collimated Holes, in California offers such a scintillation plate using terbium oxide as a constituent of the core scintillating glass. The drawback is that the scintillating glass is not as efficient as various oxide scintillating materials, and an 8 cm x 8cm x 1 cm plate costs \$80,000.

A novel concept is described in the following that can provide the advantages of high scintillation efficiency, and relatively low cost. We are able to synthesize nanoscale, unagglomerated, scintillating particles, in particular,  $\text{Lu}_2\text{O}_3:\text{Eu}$ . We have also some success with YAP:Ce. Both of these scintillate in the visible. In our laboratory, we have developed a patented aerosol combustion process by which it is possible to synthesize unagglomerated, single crystals, of complex oxides. When properly doped with rare earth elements such as Ce, Dy, Eu, etc., these crystals scintillate in the visible. By creating a coherent bundle of fibers with cores of 1 micron, and embedding scintillating particles in these cores, then the limit of resolution of the interaction of these scintillators with x-ray radiation would be of the order of 1 micron. These scintillating particles can not be placed in a collimating bundle such as made by Schott from "soft" glass, since the scintillating nanocrystallites would dissolve in the melt. We are cooperating with the Dr. Alex Argyros of the Plastic Optical Fiber group at the University of Sidney, and he is presently attempting to make a PMMA ( $n=1.5$ )/Polystyrene ( $n=1.7$ ) fiber and fiber array. We are trying techniques to achieve a uniform distribution of scintillating nanoparticles in the polystyrene core to make a coherent array in which all scintillation is confined to the 1 micron core. This would revolutionize medical imaging. We are also working with Jean Herbert and Brian Fuller of the Natick Army Materials Group. They have extrusion

equipment capable of making fibers with embedded fibers contained such that the internal fibers are 1 micron. They are using polymers for the fibers and the surrounding matrix such that their refractive indices are identical. The purpose is to obtain fiber reinforced transparent polymeric material. They plan to replace the outer or cladding polymer with a lower index material to see if guiding structures can be obtained. If these provide a light guiding matrix, then if doped with scintillating particles, this would establish, on a very small physical scale, the ability to increase x-ray resolution by the order of magnitude we claim. We have been in contact on this topic with Dr. Rox Anderson, and Dr. Rajiv Gupta of MHG. So far, there have been no "show stoppers" in our pursuit of this goal, which would be enormously important. As one example, there are certain types of breast cancer in which the precursor are small clusters involving calcified cells. These are of the order of 4-5 microns and presently undetectable.

If this can be accomplished this would, in the words of Dr. Rajiv Gupta, "revolutionize medical imaging".

### C. PMB (Polarization Mode Beating) techniques in biodetection.

#### i. Fundamentals of PMB (Polarization Mode Beating) techniques

There are many situations in which surface attachment of a molecule changes the effective refractive index of the surface, and this is the signature of the binding event. One of the best known applications is that of Surface Plasmon Resonance. The fundamental principle we wish to exploit is quite simple; however, there are practical impediments to overcome. If we wish to measure the effect of some parameter that results in a change in wavelength, orders of magnitude improvements in sensitivity can be obtained if, instead of a wavelength change, we monitor a change in frequency. Thus, the measurement is changed from the optical regime to the RF (Radio Frequency) range where simple, and inexpensive, monitoring techniques may be employed. This is, of course, especially true for perturbations that introduce a relative change in the state of a system. For example,  $\lambda \nu = C$ , where  $\lambda$ = wavelength,  $\nu$ =frequency, and  $C$ =speed of light in the medium. Therefore,  $\Delta \nu = -\frac{C}{\lambda^2} \Delta \lambda$ . With this relationship at 1,000 nm in the infra red, a frequency change of 1kHz corresponds to a wavelength shift of  $3 \times 10^{-18}$ , 3 attometer, or one millionth of a picometer. The question remains, how can this ultra-high sensitivity be achieved.

Since it is difficult to obtain a laser with stability greater than 1 MHz, heterodyning a signal with an external source is not an option. Any heterodyning with a reference signal must therefore come from the within the cavity itself. In Figure 3 we see an application of intra-cavity spectroscopy using a fiber laser. The principle is that by placing an absorber within a laser cavity, if the laser is tuned across the absorption signature, a significant decrease in output intensity will occur. This is the basis of intra-cavity spectroscopy. In Figure 4 we see the resulting influence of the presence of acetylene in the absorption cell. The ordinate is the intensity, and the abscissa is the time scale of dithering the Bragg grating in time, which corresponds to a wavelength shift.

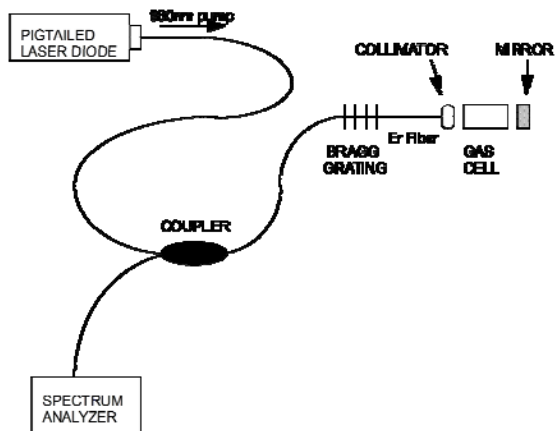


**Figure 3. Fiber Laser Intracavity Spectroscopy (FLICS)**

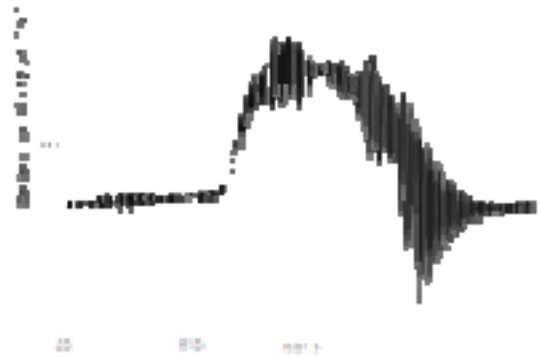


**Figure 4. Experimental tuning over an acetylene line**

This is a direct measurement of the acetylene absorption as the fiber Bragg grating is tuned by stretching. The noise in the signal is apparent.

Consider now the following. If a polarizing beam splitter is placed within the cavity as shown in Figure 5, then for a situation in which the gain is isotropic, lasing will occur in two orthogonally polarized directions, and these will be independent.<sup>i</sup>

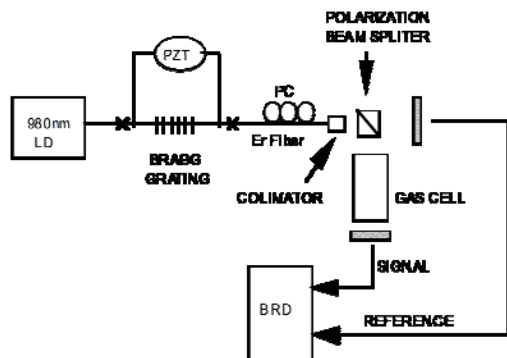


**Figure 5. Intracavity spectroscopy with independent reference arm**

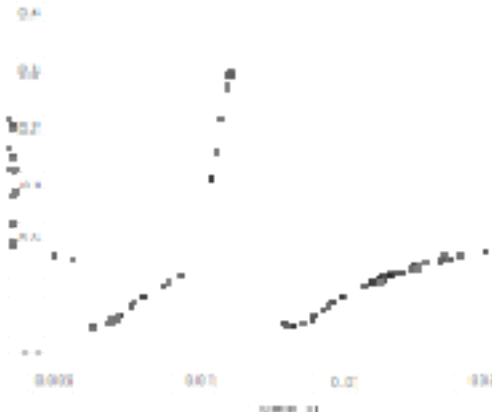


**Figure 6. Experimental tuning over an acetylene absorption line using x-y subtraction**

In Figure 6, the intensity output from both cavity arms is sent into a Newport "Nirvana" BRD (Balanced Ratiometric Detector). The optical signal is converted to an electrical signal, and the output is

$\frac{I_x - I_y}{I_x + I_y}$ , so that the result is intensity independent. The results

are shown in Figure 6, and when compared with the results of Figure 4, where there is no reference measurement, there are approximately three orders of magnitude improvement in the S/N ratio. Note the difference in ordinate scales in Figures 4 and 6. We also note the following, which is most important. In order for these measurements to have any validity, the x and y polarization components must be completely independent. If, for


example, we had used an ordinary beamsplitter in the cavity, then  $x$  and  $y$  are not independent. Internally blocking off either cavity causes the lasing on the other cavity to cease. In the case of the use of a polarization beam splitter, blocking off either cavity has no influence on the intensity output of the other cavity. They are truly independent.

This has particular significance in the measurement of ultra-small changes in wavelength by monitoring changes in frequency. We had noted above that a "narrow" laser linewidth can be of the order of a MHz. We seek to monitor much smaller changes, which can only be done by heterodyning a changing signal with a reference beam that comes from the same cavity, as in the example illustrated in Figure 2. Since we are concerned with a relative change, in this case in wavelength, all common sources of instability will be subtracted out. This includes pump noise, thermal fluctuations, vibration, etc. This is, in large measure, the explanation for the differences in Figures 6 and 4.

The question is, how can this be applied to a specific measurement? In Figure 7, we show how this concept may be used in the measurement of the optical anisotropy of a particular component inserted within the laser cavity.

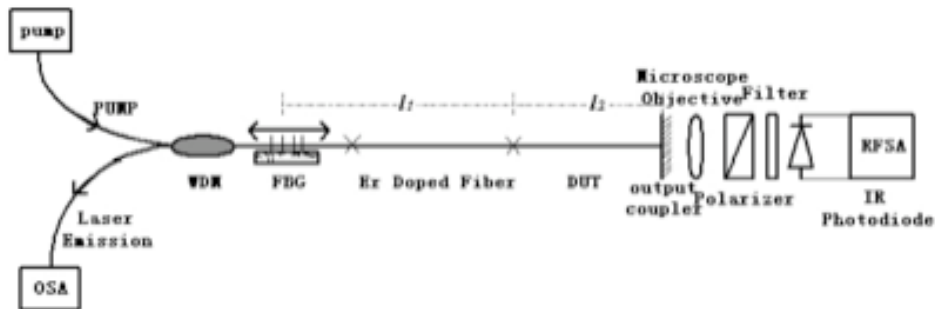


**Figure 7. Experimental arrangement to measure optical anisotropy of arbitrary photonic device.**

In this figure, with the assumption that there is no polarization anisotropy in the mirrors, or in the gain medium, and that the total anisotropy is from the component inserted in the cavity, we can obtain lasing on  $x$  and  $y$  polarization components. By projecting these onto a  polarizer, we can project these two orthogonal components onto a common axis, and the beat frequencies can be observed. These beat frequencies are the result of the optical anisotropy and may be related to the optical anisotropy. In Figure 8, we show an experimental result of introducing a PM fiber into the cavity as the DUT (Device Under Test).

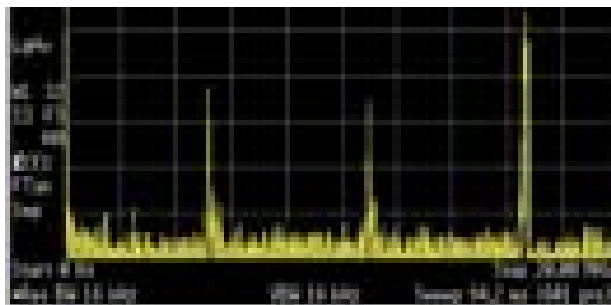


**Figure 8. RFA modal analysis shown longitudinal modes and beat frequencies**

The two symmetric modes are the modes associated with PMB (Polarization Mode Beating), and the mode on the right is a longitudinal cavity mode. The limit of sensitivity of this technique is of the order of  $\frac{\nu_x - \nu_y}{\nu_x} = \frac{2L^2}{\lambda^2} \frac{d\nu_{xy}}{d\lambda}$ , where  $\nu_x$  is the cavity frequency,  $\nu_x - \nu_y = \nu_{xy}$ , and  $L$  is the length of the anisotropic element.<sup>ii</sup> Thus, a simple measurement of the change of beat frequency with respect to wavelength provides a sensitivity of measurement that corresponds to instruments costing more than \$100,000. In addition, it is possible to measure the optical anisotropy of inserted components that have doping corresponding to the doping of the fiber laser. Other instruments can not do this.

The above method, however, does have a singular disadvantage that prevents achieving the theoretical sensitivity as indicated at the beginning of this section. This is a consequence of the fact that the cavity is not single mode, and it was necessary to perform calculations to obtain the above expression. The full sensitivity of the relation between wavelength change and frequency change can only be fully exploited in a cavity with one mode. There are several ways in which it would be possible to obtain a single mode cavity. First, the cavity could be extremely short, or, as in the case of the He laser gyroscope, the gain spectrum can be extremely narrow.

An alternate technique, that we will actively pursue and have thus far demonstrated some success, is to use a three mirror cavity, as shown schematically in Figure 9, and preliminary experiments have been performed using this configuration. An OFR (Optics for Research) mini-optical bench is used to insert the polarizing beam splitter into the cavity. There are two separate cavities that have the same isotropic gain source, a 45° polarizer insures that 1/2 of the radiation goes into each of the two polarizations within the cavity. The gain section of the fiber is 31 cm, which supports 6 longitudinal modes, and the open section of the cavity, between each of the 100% mirrors and the end of the fiber defined by the 4% reflection, is 8 cm.

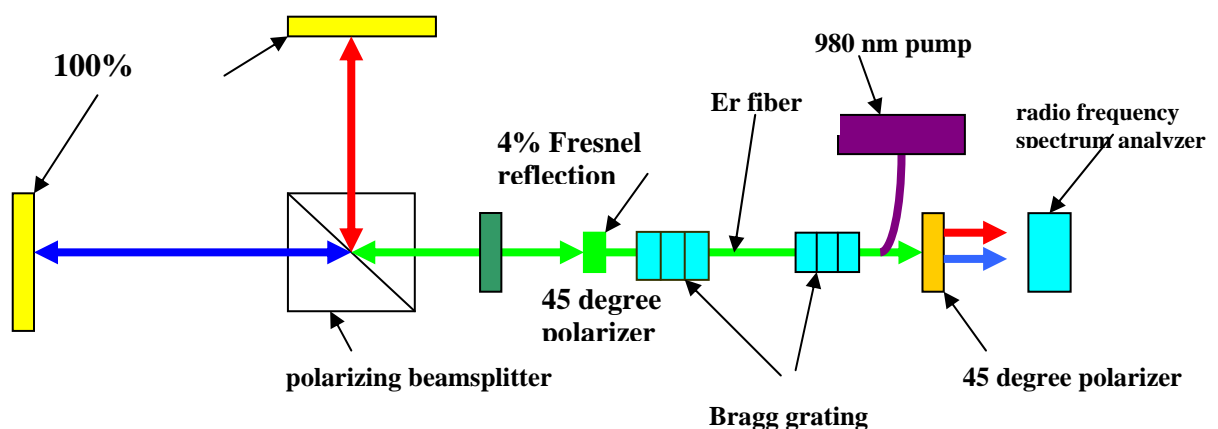
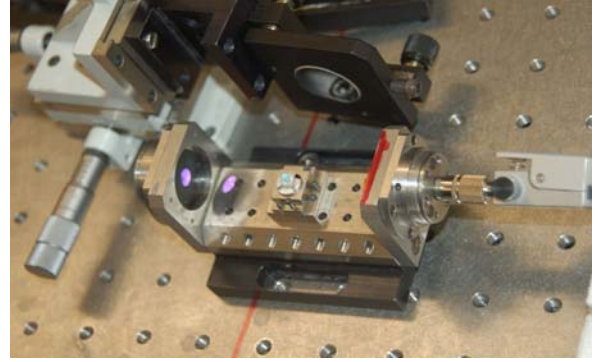


Figure 9. Schematic of PMB experiment



This length provides a single longitudinal mode. In Figure 10 we see the actual physical set-up with the polarizing beam splitter and the two cavities as schematically shown in Figure 9. When pumped at 980 nm, the modal spectrum of the 31 cm length of erbium fiber is given as shown in Figure 11. This cavity supports six modes. However, if this laser, with 4% reflection, is coupled to the OFR open cavity with a polarizing beam splitter, the additional 8 cm cavity length provides a three mirror configuration, and this shorter length is sufficient to reduce the number of modes, and only one mode oscillates. This is shown in Figure 12.



**Figure 10. OFR mini bench**

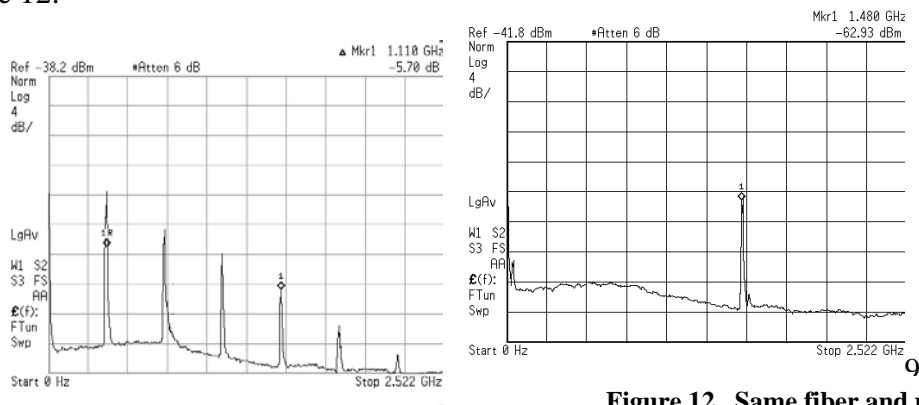


**Figure 11. Er fiber, 4% Fresnel output coupler**

**Figure 12. Same fiber and pump, with three mirror configuration, third mirror is 4% Fresnel reflection**

We have performed a simple, qualitative experiment to demonstrate the principles of polarization mode beating.<sup>iii</sup> In the configuration of Figure 9, we have inserted a soap bubble film in one polarization arm of the laser cavity. This causes a phase change in this polarization and thus allows a measurement of a relative frequency shift by measuring the change in the beat frequency with respect to the other (unchanged) polarization. The cavity is not as stable as we can make it, but, as expected, the two laser frequencies are highly correlated, so that the effect of the soap film could be readily measured as a stable frequency difference. The shift in frequency, as a consequence of the insertion of the soap film, was .4 MHz. This corresponds to a wavelength shift of only 7 femtometer. We believe that with a more stable configuration and optimizing the FWHM of the laser cavity, we can detect frequency changes that are two orders of magnitudes smaller.

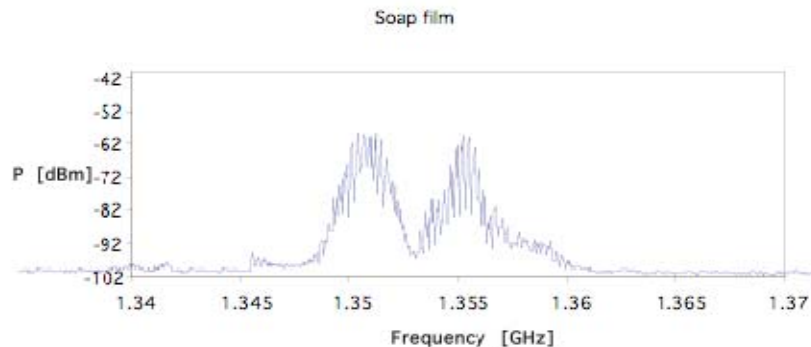


**Figure 13. Frequency shift as a consequence of the change of phase in polarization due to presence of soap film**

In addition to improvements in the FWHM of the present cavity, we will work with a He-Ne laser recently purchased from Melles Griot that will allow the insertion of a the plasma tube into a three mirror configuration and the insertion of polarizing elements, as described above, into the laser cavity. We expect this to provide significantly improved differential frequency measurements. The He-Ne laser is particularly suited for this application, since its FWHM is only 1 kHz, which should permit the detection of sub kHz frequency changes. In Figure 14 we show a measured linewidth of a He-Ne laser. The gain bandwidth of the He-Ne laser is 1.5 GHz; however, we seek to measure relative frequency changes of the order of 1 kHz, or less.

### Conclusions

The continuing interaction between the Laboratory for Lightwave Technology and the faculty at the Wellman Institute for Photomedicine will continue to be an outstanding example of symbiotic cooperation. Solving problems in modern medicine often requires a huge diversity of experience, knowledge and effort, and the Laboratory for Lightwave Technology has benefited immeasurably through introduction to new, and important problems.

### References

- 
- <sup>i</sup> . J. Hernandez-Cordero and T. F. Morse, "Gas sensors based on Fiber laser Intra-cavity Spectroscopy (FLICS)," in *Fiber Optic Sensor Technology and Applications*. SPIE proceedings Vol. 3860, Boston, MA, E.E.U.U., September 1999).
- <sup>ii</sup> Ning Li, Fei Luo, Selim Unlu, T. F. Morse, Juan Hernandez-Cordero, James Battiato, and Ding Wang, "Intra-cavity fiber laser technique for high accuracy birefringence measurements", *Optics Express*, November 2006, Vol. 14, Issue 17, pp. 7594-7603.
- <sup>iii</sup> Andrea Rosales-Garcia, Eliza Wang, Fei Luo, T.F. Morse, and Juan Hernandez-Cordero, "High Sensitivity Detection Using Intra-Cavity Mode Beating", 18th International Conference on Optical Fiber Sensors, Cancun, Mexico, October 23-27, 2006.